Ninth Canadian Conference on
Earthquake Engineering
Ottawa, Ontario, Canada
26-29 June 2007

EFFECTS OF VERTICAL EARTHQUAKE MOVEMENT ON THE DYNAMIC CHARACTERISTICS OF R/C PIER MODELS

Y. Akiyama[1], T. Okamoto[2] and I. Hirasawa[3]

ABSTRACT

The objective of this study is to clarify the effects of vertical earthquake motion on dynamic characteristics of reinforced concrete piers and to assess the degree of necessary reinforcement incase such piers receive relatively intense vertical earthquake motion in addition to horizontal earthquake motion as in an epicentral earthquake. In the experiment, horizontal earthquake motion and vertical and horizontal motions, both the simulation of the waveform of the Hyogo-ken Nanbu Earthquake, were applied to RC pier models placed on a shaking table. Specimens with twice the amount of lateral reinforcing bars were tested by the same method. The test results have revealed that the progress of visible damage to concrete is delayed. In addition, it has become clear that response displacement increases rapidly, and column becomes vulnerable to brittle failure due to buckling of longitudinal reinforcing bars. This happens because inertia force which acts on the top part of specimens fluctuates at random angles due to vertical earthquake motion, and such fluctuation results in the dispersal of sectional force generated in the base of column and damage throughout the column. Furthermore, it has been confirmed that by increasing the amount of lateral reinforcing bars, the effects of vertical earthquake motion can be inhibited.

Introduction

Japan's existing standard for the seismic design of RC bridge piers has been established based on their strength and toughness estimated through static horizontal loading tests (Japan Road Association 2002). That is because the strength and toughness of RC bridge piers have been assessed in the assumption that the material should tolerate horizontal earthquake motion. An epicentral earthquake hit the southern part of Hyogo Prefecture in 1995, and quite a few RC bridge piers were severely damaged or destroyed. Therefore, the seismic design method was thoroughly reevaluated, and numerous researches regarding the matter were conducted. Many researchers attributed the damage and collapse to the effect of horizontal earthquake motion (818gal) and the lack of toughness in those piers. Thus, those researches still focused on horizontal motion. However, the Hyogo-ken Nanbu Earthquake involved violent vertical motion (332gal) which is a characteristic of epicentral earthquakes. It is possible that a combination of horizontal and vertical motion caused the devastating damage to RC bridge piers. Therefore, we cannot ignore the impact of vertical earthquake motion when studying how RC bridge piers are damaged and how their bearing capacity decreases in an epicentral earthquake (Shimazu 2005).

[1]Leader, Chiyoda Engineering Consultants Co. Ltd., 3-C Residence Kobayashi, 8-17-10 Tegawa-cho, Kasugai-shi, Aichi-ken, Japan
[2]Graduate Student, Dept. of Civil Engineering, Chubu University, 1200 Matumoto-cho, Kasugai-shi, Aichi-ken, Japan
[3] Professor, Dept. of Civil Engineering, Chubu University, 1200 Matumoto-cho, Kasugai-shi, Aichi-ken, Japan

The object of this study is to reveal the combined effect of vertical and horizontal earthquake motions on the strength and toughness of RC bridge piers and to assess the degree of necessary reinforcement by conducting dynamic loading test. Namely we are going to introduce two types of shaking table test on RC bridge pier models simulating the seismic waveform of the Hyogo-ken Nanbu Earthquake. In one experiment, the direction of input waveform is horizontal. In the other experiment, horizontal and vertical waveforms are produced simultaneously. Then, we will compare these results in order to clarify the effect of vertical earthquake motion. Furthermore, we will introduce the same experiments conducted on test specimens which have twice as many tie bars and those with the standard number of such bars. Then, we are going to compare the results in an attempt to determine the reinforcing effect of tie bars against vertical earthquake motion.

Experimental Procedures

Experimental Program

In this research we used two kinds of specimens (Type10 and Type5) which differ in the amount of lateral reinforcing bars. In one test, horizontal shaking was applied to those specimens, and in the other vertical and horizontal shaking were applied simultaneously. That enables us to collect four types of data sets. See Table 1 for details. In order to avoid the control of the shaking table, errors in the measuring instruments, and the risk of constructional defects in the specimens and increase the reliability of the test results, 2 or 3 specimens were used for each case of the test, which amounts to 11 specimens in total.

Table 1. Experimental details.

Case title	Shaking direction	Specimen	Number of specimens
KHT10	horizontal	Type10	3
KVHT10	vertical and horizontal		3
KHT05	horizontal	Type05	2
KVHT05	vertical and horizontal		3

Test Specimens

Fig. 1 illustrates the details of RC bridge pier models used in the test. All the specimens had identical shape and measurements. The section of the piers was a 150mm X 150mm square, and the height measured from the base column was 1110mm. The span of an inertia force effect was 985mm. As for longitudinal bars, eight D10's (SD345) were used so that the ratio of reinforcing bars to piers' section would be the same as actual RC bridge piers, which is 2.54%. The tie bars used wereφ 6 (SR295) . The spacing of the tie bars for specimen Type 10 was 100mm pitch, and the tie bar ratio was 0.85%. The spacing for Type 05 was 50mm pitch, and the ratio was also 1.69%. The mechanical properties of materials are shown in Table 2. The specimens' natural frequency in the horizontal direction should be assumed approximately 5.0Hz based on authors' previous experiment in which the same type of specimens were used. The natural frequency drops down to 2.5Hz during a shaking test.

Table 2. Mechanical properties of specimen's materials.

Concrete	Specimen No.	KHT10	KVHT10	KHT05	KVHT05
Compressive stregth (MPa)	1	***	45.8	39.6	40.7
	2	49.7	41.7	35.5	36.0
	3	43.1	44.8		39.5
Modulud of elasticity (MPa)	1	***	3.40×10^4	2.57×10^4	2.73×10^4
	2	3.57×10^4	2.97×10^4	2.40×10^4	2.61×10^4
	3	2.95×10^4	3.28×10^4		2.69×10^4
Reinforcement		Longitudinal bar (D10)			
Yield strength (Mpa)		368			
Yield strain (μ)		1939			

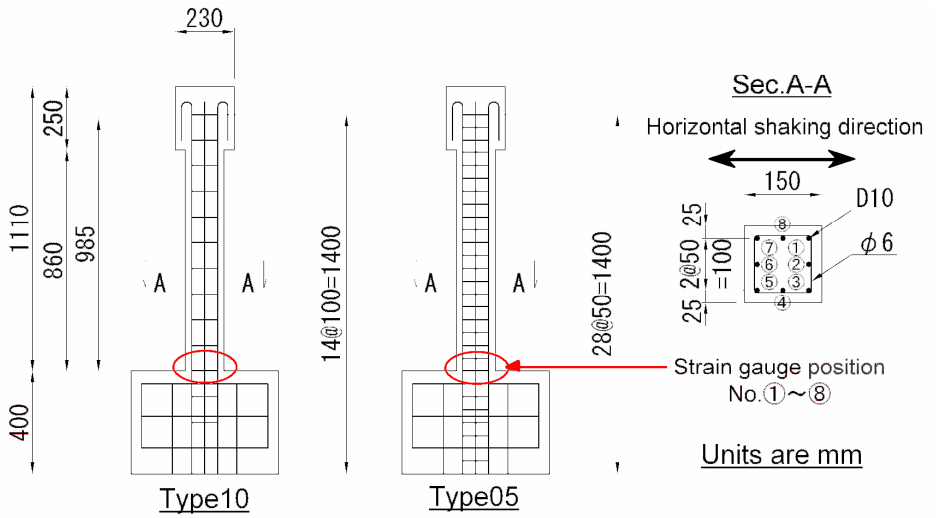

Figure 1. Details of test specimens.

Shaking Setup and Shaking Program

Shaking Setup and Instrumentation

The setting of the shaking setup, specimens, and measuring instruments for the dynamic loading test is given in Fig. 2. Specimens were fixed to the shaking table by eightφ 32 ㎜ steel rods put through their bottom part. As additional axial force or supposed superstructure reaction, a 16.2 kN spindle was placed on the top of each specimen. The axial stress at the bottom part of the specimens was 0.72 MPa.

To measure the response acceleration at the top part of the specimens, a triaxial accelerometer with the capacity of 5G was used. The response horizontal displacement at the top part was measured by a laser displacement gauge whose measuring length is -150mm ~ +150mm. Furthermore, as illustrated in Fig. 1, a strain gauge was attached to the longitudinal bars at the bottom part of each specimen so that the strain of the reinforcing bars could be measured while being shaken. A linear voltage displacement transducer (LVDT) with the gauge length of 25mm was installed to the specimens at 100mm from their bottom to measure the pulling out quantity at the bottom. In addition, a triaxial accelerometer with the capacity of 3G and a laser displacement gauge whose measuring length is -150mm ~ +150mm were installed to the shaking table in order to measure its output.

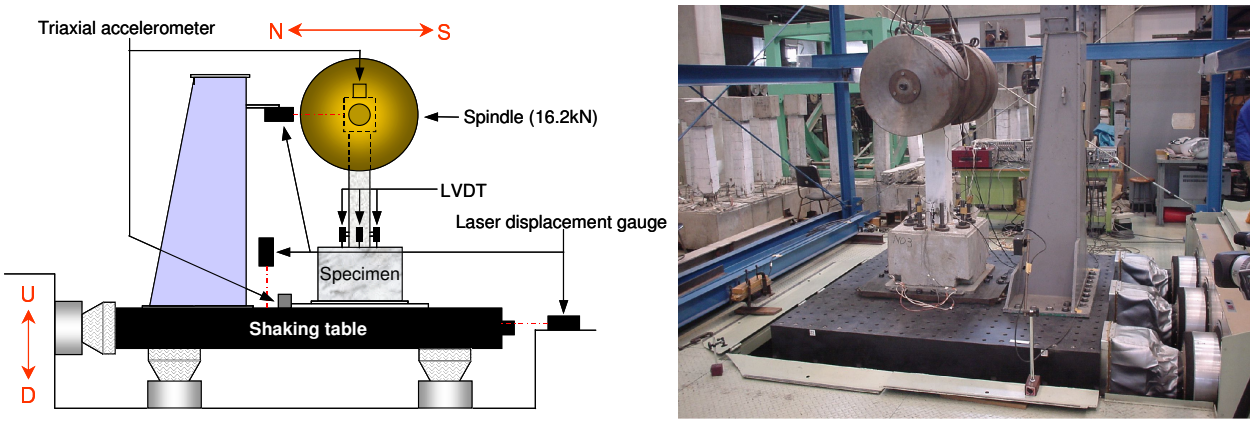

Figure 2. Loading setup.

Shaking Program

For the test, the acceleration waveform observed at Kobe Marine Meteorological Observatory at the time of the Hyogo-ken Nanbu Earthquake was used. Fig.3 shows the input waveform, and Fig.4, the vibration characteristic of the input waveform figured out through an FFT analysis. The direction of waveform shown in Fig. 3 was north-south and up-and-down. The maximum earthquake acceleration was 818 gal to the south and 332 gal upward, and the vibration period was 30 seconds. The predominant frequency of the north-south waveform was 1.3 ~ 1.8Hz as shown in Fig.4. The time scale wasn't modified.

For the loading of the seismic force, the maximum earthquake acceleration of the input waveform was increased in stages, and shaking was applied to each specimen once at each level as shown in Fig. 5. The initial input was 0.05, and input was increased by 5% each time. The shaking was conducted until the specimens were judged to reach their ultimate limit state based on the degree of damage and response displacement. That happened when the maximum earthquake acceleration was increased by 60% ~ 75%. We employed this shaking program because our objective was to assess the plastic deformation of the specimens based on envelope curves of response load and response displacement. Furthermore, as the shaking was conducted, we had to adjust the turbulence of the input waveform which was caused by the inertia force of the shaking table and specimens due to the nature of the shaking table.

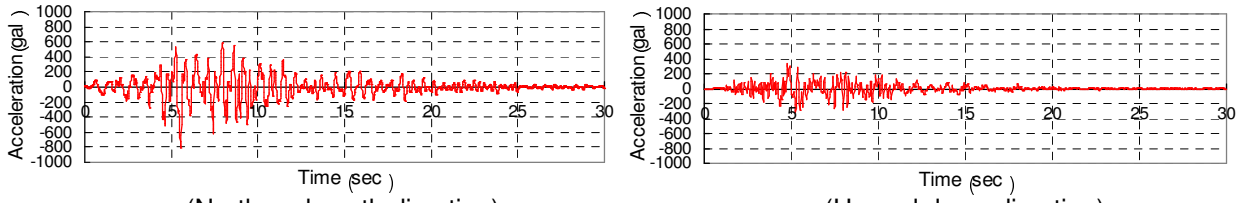

(North and south direction) (Up and down direction)

Figure 3. Input earthquake waveform.

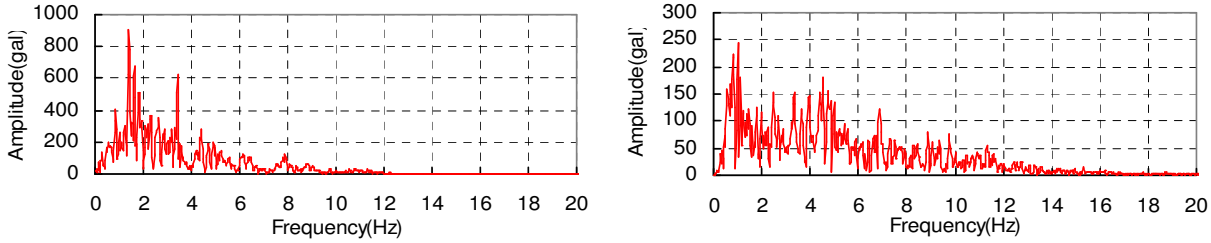

(North and south direction) (Up and down direction)

Figure 4. Vibration characteristic of the input waveform.

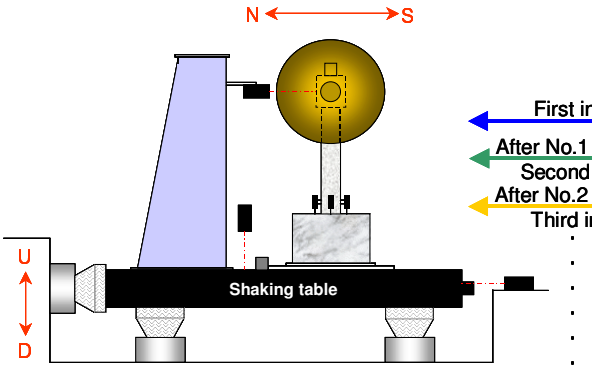

Input waveforms

First input
After No.1 shaking
Second input
After No.2 shaking
Third input

Shaking session No.	Acceleration scale	Maximum acceleration	
		N-S(gal)	U-D(gal)
1	5%	40.9	16.6
2	10%	81.8	33.2
3	15%	122.7	49.8
. . .	. . .	. . .	. . .
13	65%	531.7	215.8
14	70%	572.6	232.4
15	75%	613.5	249.0

Figure 5. Outline of shaking program.

Test Results and Discussion

In this section, among results obtained from each type of test in which 2 or 3 specimens were used, those judged to be relatively free of errors in the control of the test instruments thus the most reliable are discussed. In this research, a yield point is defined as a level of shaking during which the strain of tension reinforcement bars has reached yield strain. The tension reinforcement bars correspond to ① ~ ③ and ⑤ ~ ⑦ in Fig. 1. Resonance wasn't observed throughout the test since the natural frequency in the horizontal direction differed from the predominant frequency of the input waveform as mentioned earlier.

The Affects of Vertical Earthquake Motion

Here among the test results of KHT10 and KVHT10, the strain of longitudinal reinforcing bars, envelope curves of maximum response load – maximum response displacement, and damage to specimens' base will be compared in an attempt to reveal effects of vertical earthquake motion on RC bridge pier models.

The Strain of Longitudinal Bars

Among the strains of longitudinal bars measured at the bottom of KHT10 and KVHT 10, the maximum values of tensile strain at each level of shaking are listed in Fig. 6. KHT10 reached the yield point when shaking was increased by 45%, and KVHT, 50%. More levels of shaking were required for the specimens to reach the yield point when vertical and horizontal motions were applied simultaneously than when only horizontal motion was applied. The maximum values of tensile strain of reinforcing bars in KHT10 increased each time the level of shaking was raised. As for KVHT10, the maximum values did not really increase before reaching the yield point, and the sectional force observed at the base before reaching the yield point was weak when horizontal and vertical motions were applied. This happens because in such combined motion inertia force which acts upon the top part of the specimens is generated in an oblique direction due to the combined effect of horizontal and vertical motions, and bending moment is dispersed along column's height. In horizontal motion, inertia force is generated in a horizontal direction accordingly, and bending moment concentrates on a certain part of a column base.

The dispersal of bending moment which results from vertical earthquake motion has an advantageous effect on the base of column, provided that the maximum sectional force is taken into account in terms of seismic design. However, in elements, cut-off of longitudinal reinforcing bars for instance, which have been built based on horizontal loading and for which only the minimum sectional force has been considered, it is possible that such elements receive enormous damage due to unexpectedly strong sectional force. We need to be aware of such hazard.

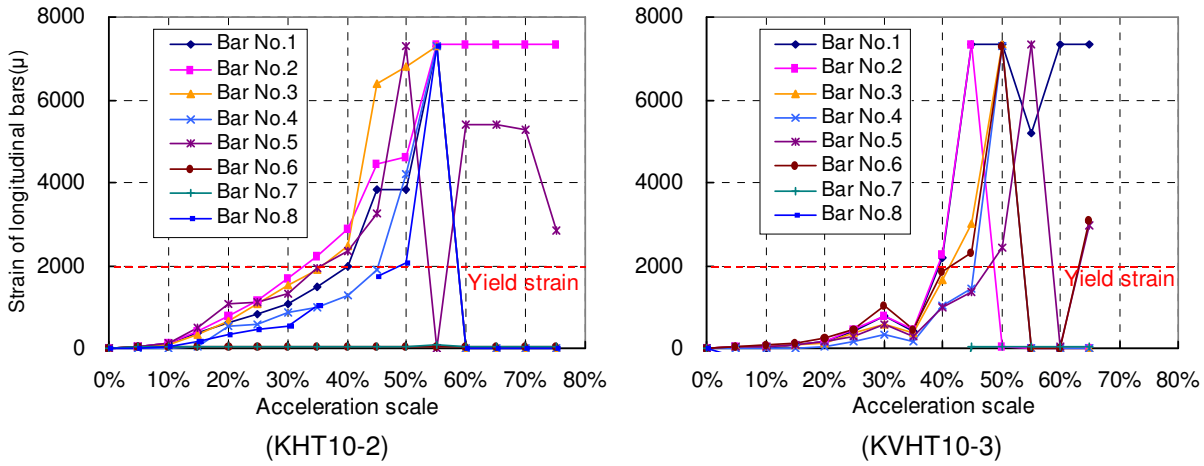

Figure 6. Maximum values of tensile strain of reinforcing bars at each level of shaking.

Envelope Curves of Response Load - Response Displacement

The vertical axis of Fig. 7 represents maximum response load obtained by multiplying response acceleration at the top part of the specimens by the equivalent load of the spindle and specimens at each level of shaking. The horizontal axis represents maximum response displacement measured at each level of shaking. Fig. 7 shows that damage caused by the excitation accumulated as the level of shaking was raised. For the purpose of relatively assessing the response of the member yielded by the waveforms, the envelope curves of average response load – average response displacement are indicated in Fig. 8. They are calculated by leveling off the plus and minus values of the envelope curves of maximum response load – maximum response displacement at each level of shaking given in Fig. 7. Table 3 shows the values of response load and response displacement at significant variation points on the envelope curves of average response.

The response load of KHT10 at yield point was 15.2kN, and KVHT10, 17.9kN. The response displacement of KHT10 at yield point was 13.0mm, and KVHT10, 18.8mm. At the maximum load point, the response load of KHT10 was 18.6kN while that of KVHT10 was 20.4kN. The response displacement of KHT10 was 24.1mm, and KVHT10, 37.4mm. These figures show that response to vertical and horizontal excitations was stronger than to horizontal excitation after reaching yield point. As shown in Fig. 8, the response displacement of KHT10 between the yield point and the ultimate limit state increased gradually over 6 shaking sessions while that of KVHT10 increased considerably within 3 sessions. Presumably, such increase in response observed after the yield point, especially displacement, reflects the difference in the progress of damage to the column bases. That is, in horizontal excitation plastic hinge was clearly formed, and hysteretic damping absorbed excitation energy. However, in vertical and horizontal excitation plastic hinge was not formed since damage to the concrete was dispersed due to the combined effect of vertical and horizontal motion. Therefore, excitation energy could not be absorbed, and the member was subject to brittle failure. Such brittle failure gives rise to a sharp decrease in the strength of RC bridge piers, and this needs to be counted when constructing an earthquake-resistant structure.

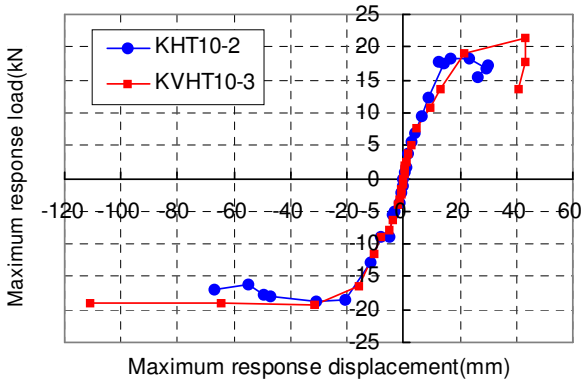

Figure 7. Envelope curves of maximum response load – maximum response displacement of KHT10 and KVHT10.

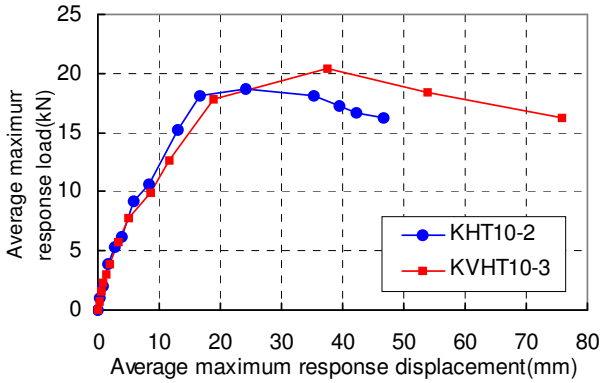

Figure 8. Envelope curves of average response load – average response displacement of KHT10 and KVHT10.

Table 3. Values of response load and response displacement at significant variation points on the envelope curves of average response of KHT10 and KVHT10.

Variation points on the envelope curves		Yield point	maximum load point	Ultimate limit
KHT10-2	Response load(kN)	15.2	18.6	16.7
	Response displacement(mm)	13.0	24.1	42.3
KVHT10-3	Response load(kN)	17.9	20.4	16.3
	Response displacement(mm)	18.8	37.4	75.8

Damage to the Base of Column

Fig. 9 is a picture of damage to the base of the specimens. Flexural cracks developed through the base of KHT10 past the yield point. After that, the crack widths increased, and cover concrete around the cracks gradually crushed as the level of shaking was raised. As for KVHT10 cracks at the base ran in an oblique direction, and an increase in crack widths was not observed. When reaching the ultimate limit state, longitudinal bars buckled, and cover concrete came off in the range of 15cm from the base. These differences in the damage state support the difference in formation of plastic hinge discussed in preceding section.

Such differences in damage progress can be attributed to a difference in the direction of inertia force effect caused by a combined effect of vertical and horizontal earthquake motion. As illustrated in Fig. 10, in horizontal motion inertia force acts horizontally only; however, in vertical and horizontal motion inertial force fluctuates at random angles. Therefore, cracks do not concentrate in one spot. Furthermore, in vertical and horizontal motion longitudinal bars buckled when reaching the ultimate limit state even though crack widths did not increase. This implies a strong possibility that inclined cracks run inside the specimens (Harada 2001). Supposedly, restraint force of cover concrete decreased due to dispersed inclined cracks, and that yielded buckling of longitudinal bars.

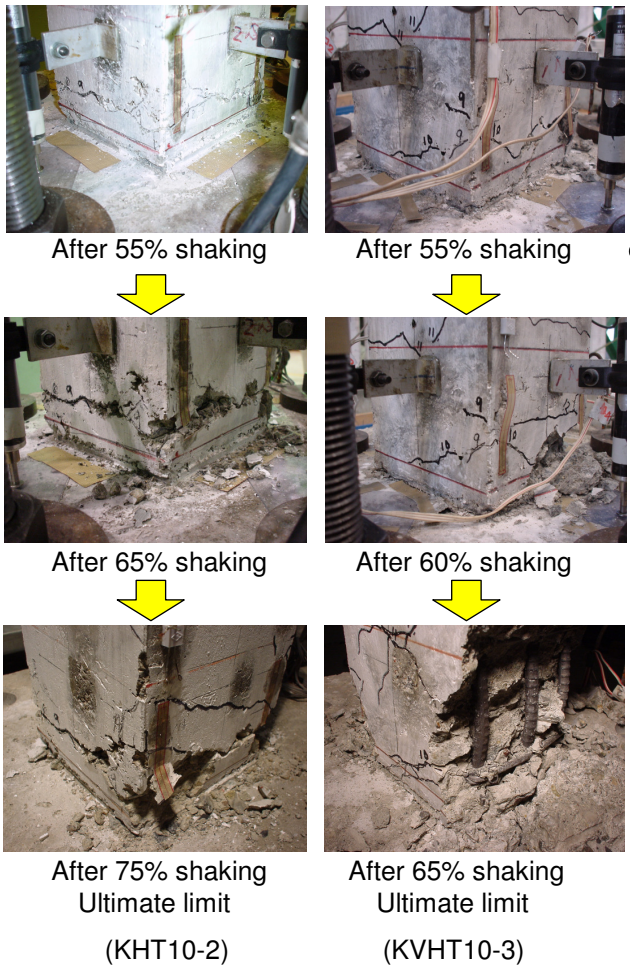

Figure 9. Picture of damage to the base of the columns of KHT10 and KVHT10.

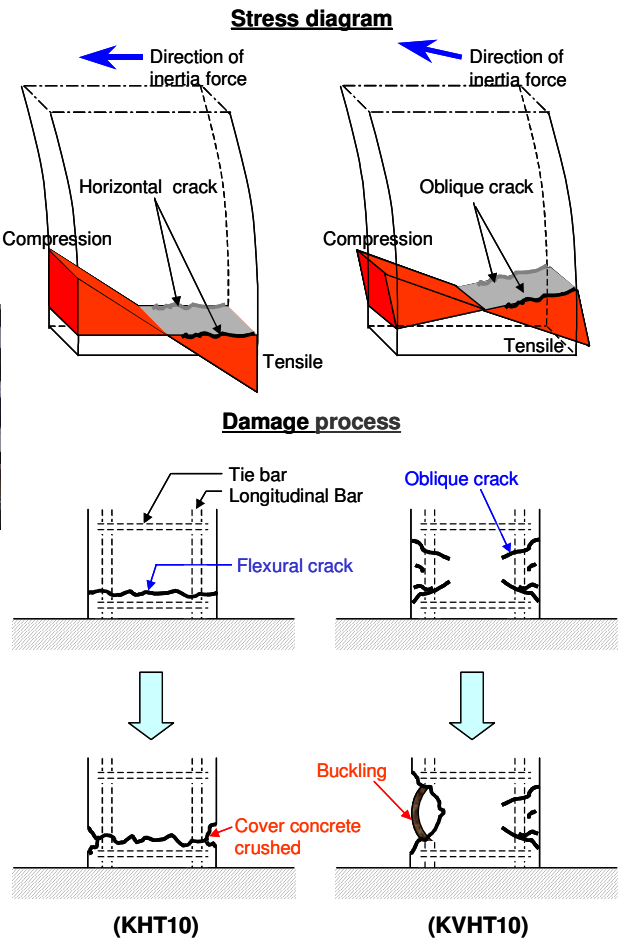

Figure 10. Mechanism of damage to the base of the columns.

Effects of Lateral Reinforcing Bars against Vertical Earthquake Motion

In this section, test results of KHT05 and KVHT05 will be compared. Furthermore, by comparing these data with the results of KHT10 and KVHT10, effects of lateral reinforcing bars against vertical earthquake motion will be examined.

The Strain of Longitudinal Bars

Among the strains of longitudinal bars measured at the bottom of KHT05 and KVHT 05, the maximum values of tensile strain at each level of shaking are listed in Fig. 11 as in Fig. 6. KHT05 reached the yield point when shaking was increased by 30%, and KVHT05, 35%. These specimens reached the yield point earlier than KHT10 and KVHT10 which both have half the amount of lateral reinforcing bars. It can be considered that bending moment caused by inertia force concentrated in the base of the specimens because the stiffness of column was magnified due to an increase in the amount of lateral reinforcing bars. With KVHT10 the maximum values of tensile strain of the reinforcing bars did not increase before the yield point; however, this was not the case with KVHT05. The maximum values increased as the level of shaking was raised. This indicates that the increase in the amount of lateral reinforcing bars inhibited the dispersal of bending moment caused by a combined effect of vertical and horizontal motion.

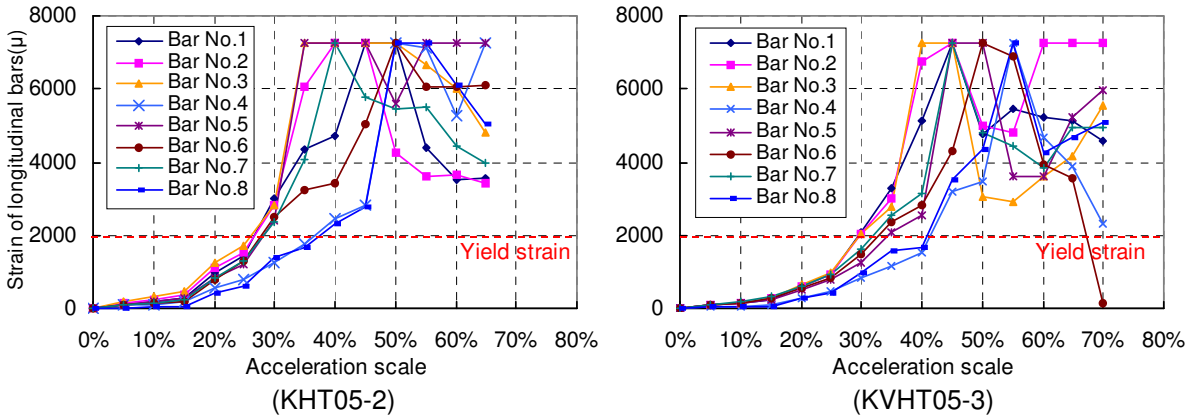

Figure 11. Maximum values of tensile strain of reinforcing bars at each level of shaking.

Envelope Curves of Response Load - Response Displacement

Fig. 12 shows the envelope carves of average response load – average response displacement of KHT05 and KVHT05. Table 4. shows the values of response load and response displacement at significant variation points on the envelope curves of average response. In Fig. 12 the envelope carves of average response load – average response displacement of KHT10 and KVHT10 are also shown for comparison.

The response load of KHT05 at yield point was 14.5kN, and KVHT05, 15.0kN. The response displacement of KHT05 at yield point was 13.0mm, and KVHT05, 12.2mm. At the maximum load point, the response load of KHT05 was 21.2kN while that of KVHT05 was 21.1kN. The response displacement of KHT05 was 31.8mm, and KVHT05, 38.6mm. Between the yield point and the maximum load there was no notable difference in response depending on the direction of the motion. As shown in Fig. 12, there was a slight difference in a tendency of envelope curves between the maximum load point and the ultimate limit state. The response load of KHT05 decreased gradually while the load of KVHT05 was maintained up to the ultimate limit state.

Comparison of the envelope curves of KHT05 and KVHT05 with those of KHT10 and KVHT10, which both have half the amount of lateral reinforcing bars has revealed some differences. When spacing between tie bars was 100mm (KHT10 and KVHT10), a difference in the envelope curves between horizontal motion and vertical and horizontal motion surfaced when response displacement past the yield point exceeded 20mm. When the spacing was 50mm (KHT05 and KVHT05), that happened when response displacement past the yield point exceeded 50mm. Considering that a difference in the amount of lateral reinforcing bars becomes apparent after longitudinal reinforcing bars reached the yield point, it can be said that effects of vertical earthquake motion are related to an amount of lateral reinforcing bars. In addition, by providing a sufficient amount of lateral reinforcing bars, effects of vertical earthquake motion on the shape of envelopes can be reduced.

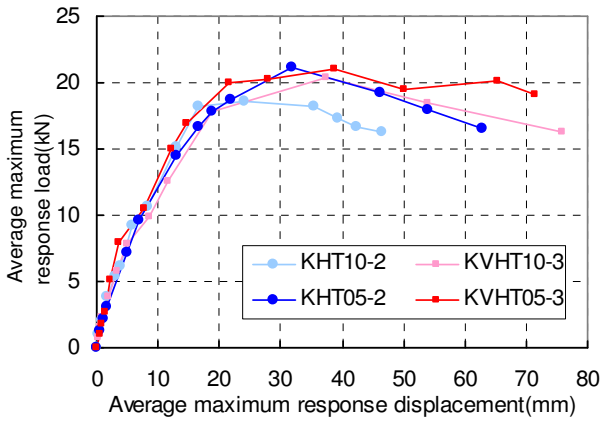

Figure 12. Envelope curves of average response load – average response displacement of KHT05, KVHT05 and KHT10, KVHT10.

Table 4. Values of response load and response displacement at significant variation points on the envelope curves of average response of KHT05 and KVHT05.

Variation points on the envelope curves		Yield point	maximum load point	Ultimate limit
KHT05-2	Response load(kN)	14.4	21.2	16.5
	Response displacement(mm)	13.0	31.8	62.8
KVHT05-3	Response load(kN)	15.0	21.1	19.1
	Response displacement(mm)	12.2	38.6	71.3

Damage to the Base of Column

Fig. 13 is a picture of damage to the base of KHT05 and KVHT05 in their ultimate limit state. In KHT05 cracks ran horizontally. Furthermore, the widths of cracks in a tensile side increased, and cover concrete in a compression side crushed. As for KVHT05 cracks at the base ran in an oblique direction, but the buckling of longitudinal reinforcing bars and delamination of cover concrete were not observed unlike KVHT10.

(KHT05-2)

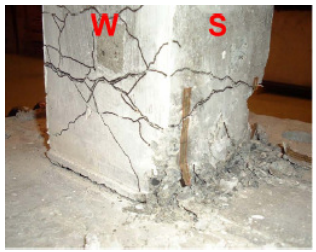

(KVHT05-3)

Figure 13. Picture of damage to the base of the columns of KHT05 and KVHT05.

As seen in KHT05, the widths of cracks in a tensile side increased, and cover concrete in a compression side crushed. It has been revealed that inclined cracks develop due to a combined effect of vertical and horizontal earthquake motion even though a sufficient amount of lateral reinforcing bars are used. Nevertheless, the progress of damage caused by buckling of longitudinal reinforcing bars can be inhibited. In KHT05 to which horizontal motion was applied, plastic hinge was not formed, either. The amount of lateral reinforcing bars used (the ratio was 1.69%) must have led to an excessive restraint effect. These findings suggest that it is desirable to use as many lateral reinforcing bars as possible within the range of

design standard in order to construct a structure resistant to vertical earthquake motion.

Conclusions

In order to reveal influence of a combined effect of vertical and horizontal motion on the dynamic characteristics of RC bridge piers and to examine the effectiveness of lateral reinforcing bars against such influence, a dynamic loading test was conducted. In the test, 2 types of excitation, horizontal motion and vertical and horizontal motion, were applied to RC bridge pier models placed on a shaking table. Based on the test, the following conclusions have been drawn:

1. By measuring tensile strain of longitudinal reinforcing bars, it has become clear that less sectional force is generated in the base of column up to the yield point when vertical and horizontal motions are applied simultaneously than when horizontal motion is applied.
2. The envelope curves of maximum response load – maximum response displacement of the top part of the specimens and the damage state of the base indicate that plastic hinge is not formed, and excitation energy is not absorbed in vertical and horizontal motions. This is because cracks in the base of column run in an oblique direction and damage does not concentrate in the base. Consequently, brittle failure results at the ultimate limit state as well as buckling of longitudinal reinforcing bars.
3. The dynamic characteristics of RC bridge pier models mentioned in (1) and (2) are attributed to a certain factor. That is, the inertia force, which acts on the top part of the column, fluctuates at random angles due to a combined effect of vertical and horizontal motion; consequently, sectional force and damage in the base of column disperse throughout the column. In order to build earthquake-resistant RC bridge piers, sectional force of the cut-off of longitudinal reinforcing bars and the hazard of a sharp decline in strength of column caused by brittle failure at the ultimate limit state need to be considered.
4. The measuring result of tensile strain of longitudinal reinforcing bars obtained from shaking table test on specimens with twice amount of lateral reinforcing bars supports that dispersal of sectional force can be reduced. In addition, judging from the envelope curves of response load – response displacement and damage state of the base column obtained from the test, it is possible to inhibit brittle failure at the ultimate limit state. The spacing of lateral reinforcing bars which prevented the buckling of longitudinal bars was five times wider than that of longitudinal bar diameter.
5. (4) suggests that by using as many lateral reinforcing bars as possible, within the range of design standard, effects of vertical earthquake motion on RC bridge piers can be inhibited.

References

Japan Road Association, 2002. *Specifications for Highway Bridges Part V Seismic Design*, Maruzen,Tokyo,Japan.

Shimizu, T., 2005. On the Characteristics of Vertical Ground Motions Induced by Earthquakes and the Seismic Provisions regarding Vertical Ground Motions in Each Building Code of Japan,China and U.S.A., *Concrete Journal* 43 (482), 12-17.

Harada, K., N. Ishikawa, S. Katsuki and T. Ohta, 2001. Dynamic Lateral Resistance of Reinforced Concrete Short Column Model with Circumferential Crack Caused by Impulsive Uplift Load, *Concrete Research and Technology* 12 (26), 27-40.